Electronic structures of cyclometalated palladium complexes in the higher oxidation states

Bao N. Nguyen,[a] Luis A. Adrio,[a] Tim Albrecht,[a] Andrew J. P. White,[a] Mark A. Newton,[b] Maarten Nachtegaal,[c] Santiago J. A. Figueroa,[b] and King Kuok (Mimi) Hii[a,]*

[a] Department of Chemistry, Imperial College London, South Kensington, London SW7 2AZ, U.K. [b] European Synchrotron Radiation Facility, 6 rue Jules Horowitz, 38000 Grenoble, France. [c] Paul Scherrer Institut, 5232 Villigen PSI, Switzerland.

General experimental conditions for the preparation of palladium complexes and catalytic reactions. All reactions with air- or moisture-sensitive materials were carried out under N_2 using standard Schlenk techniques. Anhydrous solvents were dried by passing through molecular sieves under N_2 in purification towers. Unless otherwise stated, all chemical reagents and precursors were procured from commercial sources and used without purification. Complexes **1-4**,[1-4] were prepared according to reported methods and their characterisation data verified with literature values.

Acetoxylation of 2-phenylpyridine (1) using $PhI(OAc)_2$ as an oxidant. A oven-dried vial under nitrogen was charged with 2-phenylpyridine (100 mg, 0.64 mmol.), $Pd(OAc)_2$ (14.0 mg, 0.062 mmol.), $PhI(OAc)_2$ (216 mg, 0.67 mmol.) and anhydrous acetonitrile (2 mL). The vial was sealed under N_2 and heated at 100 ºC overnight. Solvent was then evaporated and the reaction purified using flash chromatography (Et_2O:light petroleum = 1 : 9) to give the expected product (55 mg, 40% yield). The characterisation data (NMR, mpt and IR) match that reported in literature.

X-ray crystallography.

Crystals of compound **3** and **4** suitable for X-ray crystallography were obtained by slow diffusion of hexane into a solution of the complex in dichloromethane and chloroform, respectively, at –20 ºC.

Crystal data for 3: $C_{22}H_{16}N_2Pd{\cdot}0.5(CH_2Cl_2)$, M = 457.23, orthorhombic, *Pbcn* (no. 60), a = 10.9858(3), b = 15.3568(3), c = 22.4969(4) Å, V = 3795.38(14) Å^3, Z = 8, D_c = 1.600 g cm^{-3}, μ(Mo-Kα) = 1.127 mm^{-1}, T =

173 K, pale yellow plates, Oxford Diffraction Xcalibur 3 diffractometer; 6230 independent measured reflections (R_{int} = 0.0325), F^2 refinement,[5] R_1(obs) = 0.0566, wR_2(all) = 0.1282, 4756 independent observed absorption-corrected reflections [$|F_o| > 4\sigma(|F_o|)$, $2\theta_{max}$ = 65°], 267 parameters. The crystal structure data has been deposited at the Cambridge Crystallographic database (ref: CCDC 905536).

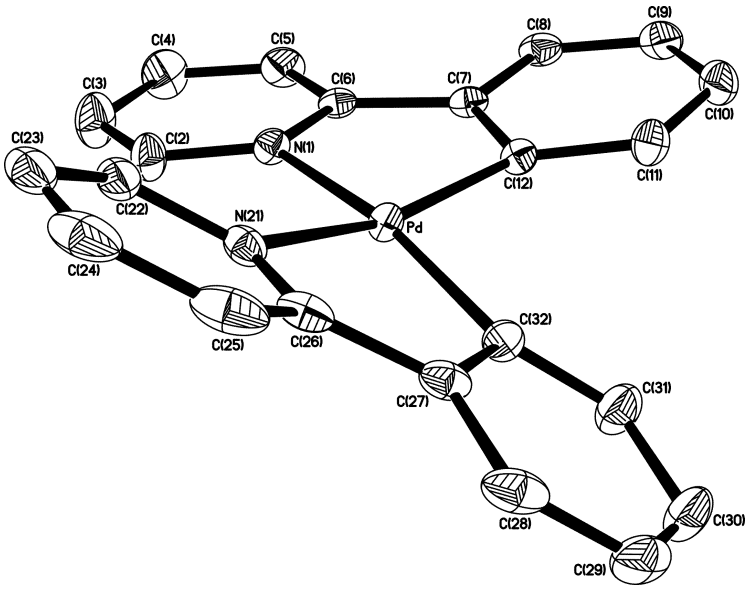

Fig. S1. The crystal structure of **3** (30% probability ellipsoids).

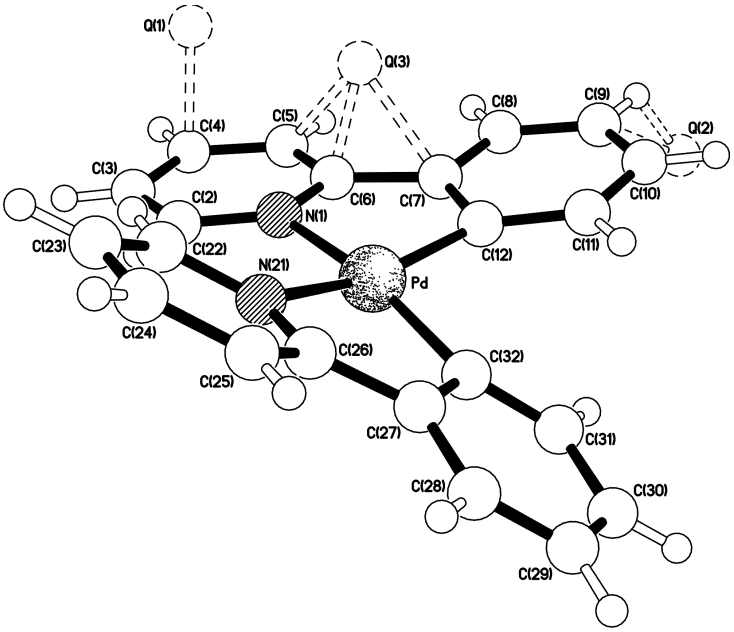

Fig. S2 The crystal structure of **3** showing the three largest residual electron density peaks, Q(1), Q(2) and Q(3) (of *ca*. 2.44, 1.69 and 1.40 eÅ^{-3} respectively).

Table S1. Comparative selected bond lengths (Å) and angles (°) for **3**, INEVIG and MIXKUZ (both independent molecules).[a]

3	INEVIG	MIXKUZ-A	MIXKUZ-B

Pd–N(1)	2.121(3)	2.13(1)	2.121(5)	2.132(5)
Pd–C(12)	1.992(4)	1.99(1)	1.999(6)	1.990(6)
Pd–N(21)	2.136(3)	2.11(1)	2.109(5)	2.110(5)
Pd–C(32)	1.993(4)	2.00(1)	1.982(6)	2.009(5)

[a] The atom labelling for the literature structures have been adjusted to match that of **3** (see Fig. S1).

The crystal structure of **3** (Fig. S1) shows the expected twisted square planar coordination of two phenylpyridine ligands to the palladium centre, the two [Pd,N,C] coordination planes being inclined to each other by *ca*. 24°. The coordination distances for the two ligands are very similar to each other, with the Pd–N bond length being ca. 0.13 Å longer than its Pd–C counterpart in both instances. Only two crystal structures of 4-coordinate (phenylpyridine)palladium complexes have previously been reported, INEVIG[6] and MIXKUZ;[7] these complexes have one or two of the phenyl rings π-bound to $Cr(CO)_3$ units respectively.[8,9] The structure of the complex with one $Cr(CO)_3$ unit (INEVIG) is unfortunately of low quality, the estimated errors in the bond lengths being ca. 0.01 Å for the coordination distances and *ca*. 0.02 Å for the bonds within the aryl rings. As such, few meaningful comparisons can be made, though the Pd–N distances are still markedly longer than their Pd–C counterparts [Pd–N 2.13(1) and 2.11(1) Å, cf. Pd–C 1.99(1) and 2.00(1) Å, Table S1]. The structure of MIXKUZ, with both phenyl rings π-bound to $Cr(CO)_3$ units, contains two independent molecules, and both of show the same pattern of bond lengths for the coordination distances as seen in 2 (Table S1).

The most noticeable feature of the determination of this structure is the presence of three residual electron density peaks that are significantly larger than the rest, the top six in order being *ca*. 2.44, 1.69, 1.40, 0.65, 0.54 and 0.52 $eÅ^{-3}$. These three peaks (labelled Q(1), Q(2) and Q(3) respectively in Fig. S2) lie in positions that are neither chemically sensible, nor fit to any discernible disorder pattern. One obvious possible cause for such peaks is twinning. Though by eye there were no signs of multiple overlaid orientations for the crystal studied, it was evident that the crystal had suffered some internal damage before being introduced into the low temperature stream (a number of internal cracks were evident in all of the crystals in the sample.) However, in spite of this apparent damage, instead of being the expected diffuse streaks the diffraction spots were surprisingly well formed, and the indexing of the complete data set did not reveal any significant twinning, with *ca*. 93% of the observed diffraction spots fitting to the reported unit

cell. Without any better explanation, however, it still seems most likely that these three anomalously large residual electron density peaks are due to some unresolved twinning, and so would not represent “real” electron density present in the structure.

The positions of the nitrogen atoms of the two phenylpyridine rings [*i.e.* N(1) and N(21)] were determined by comparison of the thermal parameters and aryl ring bond lengths involving the two possible sites in each ligand when they were both refined as carbon atoms (it was assumed that the nitrogen centre would be coordinated to the palladium). *R*-factor tests for each site separately refined as carbon or nitrogen also convincingly supported the assignments.

The included dichloromethane solvent molecule was found to be disordered across a C_2 axis. Two unique orientations of *ca*. 42 and 8% occupancy were identified for the whole molecule, with two further orientations of the same occupancies being generated by operation of the C_2 axis. The geometries of the two unique orientations were optimised, the thermal parameters of adjacent, chemically equivalent, atoms were restrained to be similar, and only the non-hydrogen atoms of the major occupancy orientation were refined anisotropically (the remainder were refined isotropically).

Crystal structure of 4: $C_{26}H_{22}N_2O_4Pd{\cdot}3CHCl_3$, M = 890.96, triclinic, P-1 (no. 2), a = 9.26266(13), b = 12.1740(3), c = 16.6694(3) Å, α = 85.1400(19), β = 87.1778(14), γ = 70.4519(19)°, V = 1764.55(6) Å^3, Z = 2, D_c = 1.677 g cm^{-3}, μ(Mo-Kα) = 1.245 mm^{-1}, T = 173 K, pale yellow blocks, Oxford Diffraction Xcalibur 3 diffractometer; 11645 independent measured reflections (R_{int} = 0.0176), F^2 refinement,[5] R_1(obs) = 0.0355, wR_2(all) = 0.0882, 9352 independent observed absorption-corrected reflections [$|F_o| > 4\sigma(|F_o|)$, $2\theta_{max}$ = 66°], 408 parameters. The crystal structure data has been deposited at the Cambridge Crystallographic database (ref: CCDC 948332).

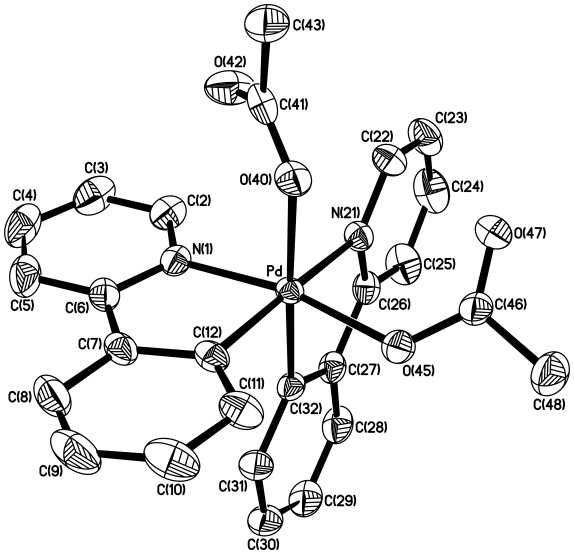

Fig. S3 The crystal structure of **4** (50% probability ellipsoids).

Table S2. Comparative selected bond lengths (Å) and angles (°) for **4**, LUFQOT and QAVCAS.[a]

	4	**LUFQOT**	**QAVCAS**
Pd–N(1)	2.0247(17)	2.033(2)	2.019(2)
Pd–C(12)	1.9995(18)	2.004(3)	2.019(2)
Pd–N(21)	2.1501(16)	2.154(3)	2.138(2)
Pd–C(32)	2.0015(18)	1.985(4)	2.013(3)
Pd–O(40)	2.1650(13)	2.106(2)	2.087(2)
Pd–O(45)	2.0183(14)	2.017(3)	2.0394(19)

[a] The atom labelling for the literature structures have been adjusted to match that of **3** (see Fig. S2).

The positions of the nitrogen atoms of the two phenylpyridine rings [*i.e.* N(1) and N(21)] were determined by comparison of the thermal parameters and aryl ring bond lengths involving the two possible sites in each ligand when they were both refined as carbon atoms (it was assumed that the nitrogen centre would be coordinated to the palladium). *R*-factor tests for each site separately refined as carbon or nitrogen also convincingly supported the assignments.

Three X-ray crystal structures of *bis*(phenylpyridine)palladium complexes with two oxygen donor ligands have previously been reported; in each case the oxygen donors are carboxylate groups. The two ordered structures (LUFQOT[3] and QAVCAS[10]) both have asymmetric octahedral metal centres with one carboxylate group *trans* to a nitrogen donor and the other carboxylate group trans to a carbon donor (as is seen for **3**, Fig. S2). In neither literature case are any details given as to how the nitrogen atom of each phenylpyridine ligand was located. However, as (i) the structures have not been modelled with any disorder,

(ii) the thermal parameters of the donor atoms look mostly reasonable (though those of the N1-based phenylpyridine ligand in LUFQOT show some rocking), and (iii) the pattern of the bond lengths around the donor atoms is similar to that that seen for **4** (Table S2) we believe the nitrogen atom positions to be reliable.

However, the third literature structure (LUFQIN[3]) has a C_2 axis through the metal centre, requiring the octahedral metal centre to be symmetric. This structure has been modelled with a 50:50 disorder of the position of the nitrogen donor within the unique phenylpyridine ligand, and this allows the asymmetric structure as a possibility. Unfortunately, neither the paper nor the accompanying supporting information gives any details about the crystallography, so we cannot tell why the authors thought it was necessary to invoke the presence of this disorder, nor how they handled it. Inspection of the CIF file, particularly the thermal parameters and coordination distances of the donor atoms of the unique phenylpyridine ligand, suggest no reason for the modelling of any disorder. The only indication of some potential swapping of the carbon and nitrogen positions is a lack of a clear asymmetry in the bonds to the donor sites within the aryl rings; in **4**, the N(donor)–C_{Ar} distances are *ca*. 0.04 Å shorter than their C(donor)–C_{Ar} counterparts. It is worth noting at this point that the authors have modelled the disorder in LUFQIN by having the alternate donor atoms at exactly the same coordinates, which **4** and the ordered structures LUFQOT and QAVCAS all show is unrealistic. Additionally, LUFQIN shows no elongation of the thermal ellipsoids of the donor atoms along the bonds to the palladium which would be expected to be observed if there were an overlay of two different coordination distances. Given the uncertainty caused by the disorder, the lack of explanation as to why the structure was thought to be disordered, and the manner in which the disorder was modelled, LUFQIN is not a suitable structure for comparison.

Comparative coordination distances for the structures of **4**, LUFQOT and QAVCAS are given in Table S2, and show that the Pd–N distances are much more affected by the *trans* atom than the Pd–C distances. Whilst the Pd–N distances trans to carbon [Pd-N(21)] are *ca*. 0.12 Å longer than those where the nitrogen is *trans* to oxygen [Pd-N(1)], the Pd–C distances are almost unaffected (ranging between 1.985(4) and 2.019(2) Å].

XAS measurements.

XAS measurements were performed at the SuperXAS beamline at the Swiss Light Source (SLS, Villigen, Switzerland). The ring was operated in top-up mode with 400 mA of 2.4 GeV electrons. The beam was collimated by a Pt-coated mirror and then monochromatised using a double crystal monochromator equipped with two Si(111) crystals. The X-ray beam was focused down to a size of 100 x 100 μm^2 by means of toroidal Pt mirror placed downstream of the monochromator. Samples were measured in transmission mode at the K-edge of Pd (24. 35 keV) in a continuous scanning mode using ionization chambers filled with an argon-nitrogen gas mixture. Energy calibration was performed using a Pd metal foil.

Further XAFS experiments were conducted on the bending magnet beamline BM23 at the European Synchrotron Radiation Facility (ESRF, Grenoble, France). The storage ring conditions were 6 GeV, operating in uniform mode between 150-200 mA. The measurements were performed using a Si(111) monochomator (2.0 x 10^{-4} $\Delta E/E$), and Pt mirrors were used to eliminate higher harmonics in the beam. Three ionization chambers are filled with optimal He/Kr gas mixture at a total pressure of 2 bars, in order to have an absorption of 30% in I_0 and 70% in I_1 and I_2 at the Pd K-edge. The spectra were collected in transmission mode. The monochromator was calibrated with a Pd foil and we constantly monitored the spectra of such foil in transmission in order to account for small energy shifts (<1 eV) during the measurements. The primary vertical exit-slit size was fixed at 0.2 mm, and the horizontal experimental slit size was adjusted to 0.7 mm. The pre-edge region was scanned with 4 eV steps. Along the edge the step size was reduced to 0.4 eV in order to obtain the adequate resolution for the X-ray absorption near edge structure (XANES).

Sample preparation for EXAFS experiments: Solid samples where pressed into 10 mm discs using cellulose powder as a matrix. Solutions of complexes **1** and **3** were recorded in solution in 1,2-dichloroethane (60 mM and 40 mM, respectively) using scanning mode at palladium K-edge using a quartz cuvette (10 mm path-length). For higher oxidation state complexes **2** and **4**, the oxidant $PhI(OAc)_2$ (1 eq.) was added to the solution of the palladium complex (**1** or **3**, respectively) in 1,2-dichloroethane in a round-bottom flask with stirring at room temperature. After 10 minutes, it was transferred to a syringe and mounted in the beamline. Spectra were collected after 10 minutes. Each scan took about 120 seconds and

15-20 scans were collected on each sample before significant decomposition can be detected. No formation of Pd black was observed within the timescale of these experiments.

The time required to generate the oxidative adducts were established by off-line NMR experiments: To a solution of complex **1** (5 mg) in $CDCl_3$ (0.6 mL) at room temperature was added $PhI(AcO)_2$ (5 mg, 1 eq.). Rapid mixing was associated with immediate colour change from yellow to dark orange. ^1H NMR showed complete disappearance of starting material and formation of the product which was stable over at least 40 minutes. The conversion of complex **3** to **4** was also extremely rapid (<30 minutes).[3] The resultant complex **4** was found to be sufficiently stable over the timescale of the spectroscopic experiment (< 2 hours).

Data processing and fitting were performed using FEFF6 theory and the non-commercial package IFEFFIT developed by Ravel and Newville.[11] All spectra are calibrated against Pd foil (E_0 = 24.35 keV). After background subtraction, FT was carried out over *k*-range = 2-15.3, no phase-corrections were applied. Solid structure of compound **1** and **3** were used to calibrate fitting and to determine the S02 value for the first shell. Fits were obtained using S02 = 0.76 – 0.77 for compounds **1** and **3**. For the oxidised solution of **2** and **4**, S02 was set 0.84 and 1.07, respectively. This was due to the transient nature of these species, which led to shorter data collection time and the present of other species in solution.

Additional information inserted during revision process, in response to reviewer's comment: The data collected for complex **3** (solid-state) shows minimal disorder in the first coordination shell. The fit is actually better than it seems visually, with R-factor value at 0.2%. However, it was only performed for radial distance between 1 and 2 Å to address the first shell (Pd-C and Pd-N bond lengths at 2.14 and 1.99 Angstroms). Further scatterers and multiple-scattering are not included given the quality of the data (background peak at radial distance at 1 Å). It is possible that partial sample decomposition contributed to the poor quality of the data of this complex.

Raw data for EXAFS experiments are available to download at:

http://dx.doi.org/10.6084/m9.figshare.1513788

X-ray beam damage of complex **4** may be illustrated by the following spectra, collected consecutively over 10 scans. There were little changes in the edge jump, although the normalised spectra showed some slow

changes. Thus, there were some decomposition while the sample over 10 scans, but it is not possible to attribute this entirely to X-ray beam damage, as the formation of Pd nanoparticles not evident in the pathlength within the cuvette, which is normally the case.

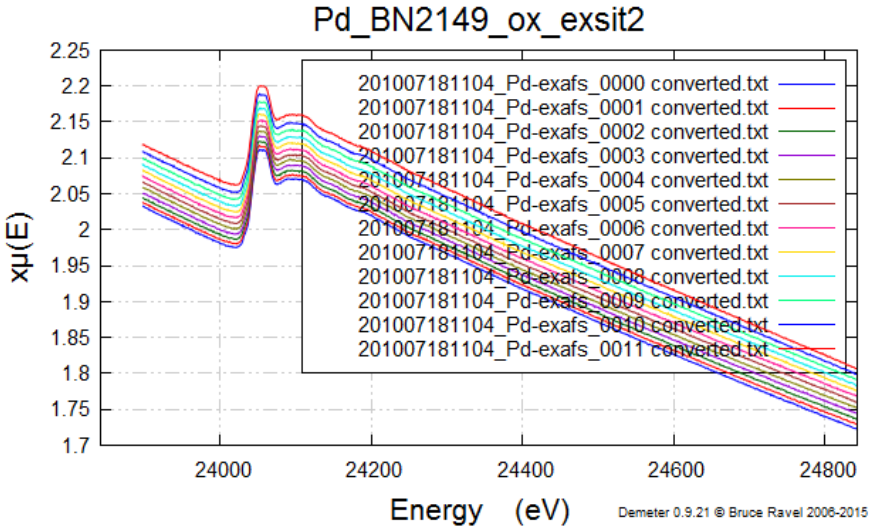

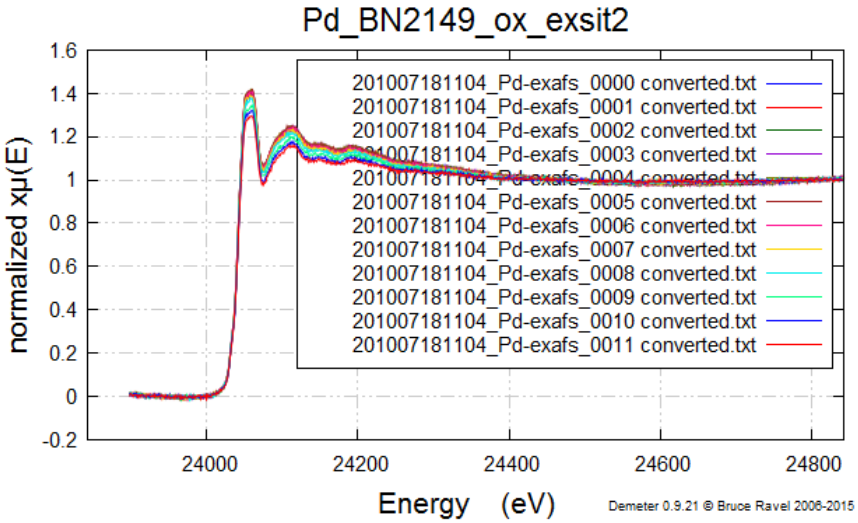

EXAFS analyses:

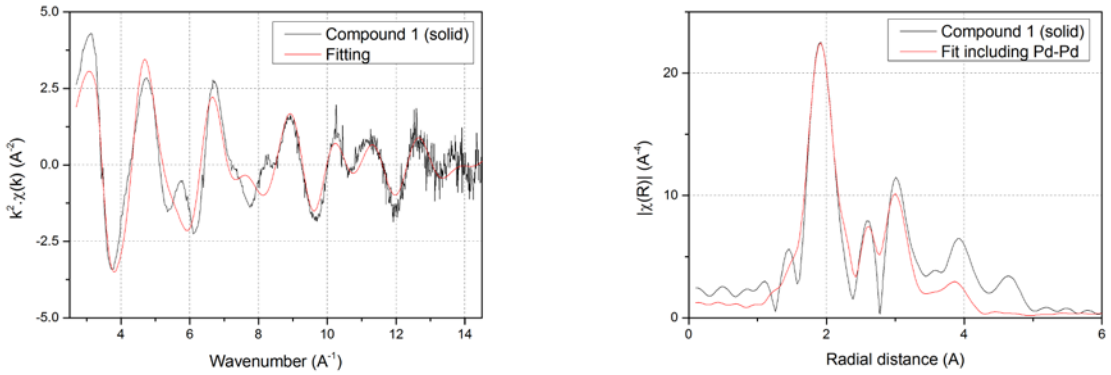

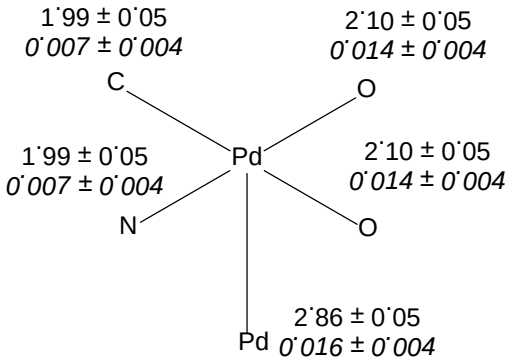

S02	= 0˙77
CN	= 5
E0	= 5˙22
R-factor	= 0˙61

Figure S4. Fit of structure **1** (first shell of solid data), R-range 1-3.5, using EXCURV98. Bond distances are in Å in normal font, Debye-Waller factors are in italic font. The *trans* structure of the dimer was used for the fit, although a mixture of *cis* and *trans* isomers could also be present.

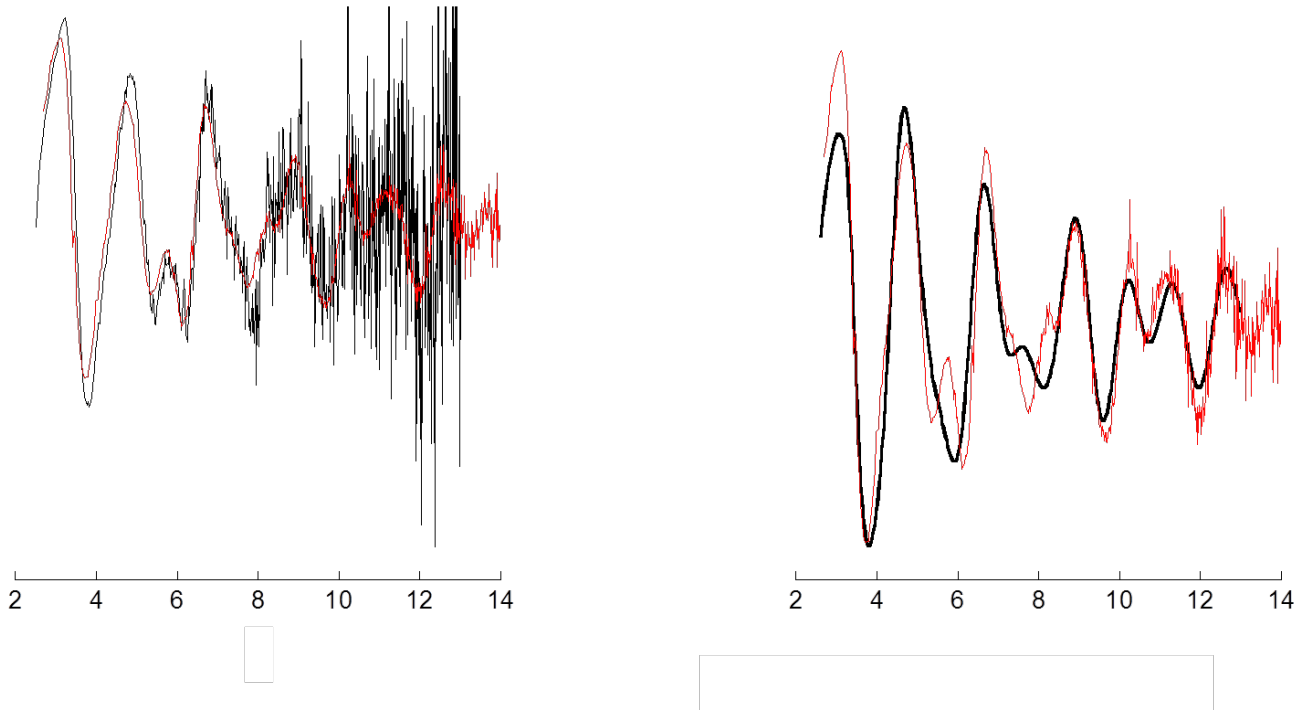

Figure S4A. Fit of structure **1** as a sample in solution (dichloroethane): Left – Comparison of raw k^3 EXAFS (red = solid, black = solution). Right: Comparison of raw k^3 EXAFS (red = solid, black = solution after applying 5 point smoothing).

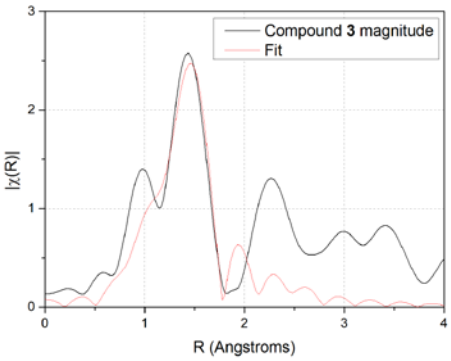

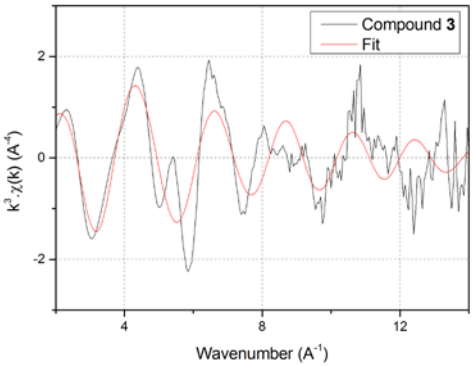

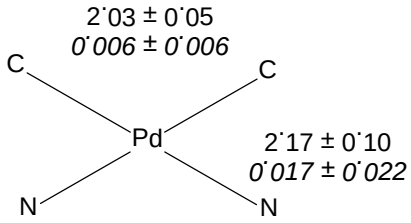

S02	= 1.03 (different beamline)
CN	= 4.1
E0	= -4.24 ± 2.63
R-factor	= 0.002

Figure S5. Fit of structure **3** (solid-sample, first shell of *cis* isomer using crystal structure), R-range 1-2, using Demeter. Bond distances are in Å in normal font, Debye-Waller factors are in italic font.

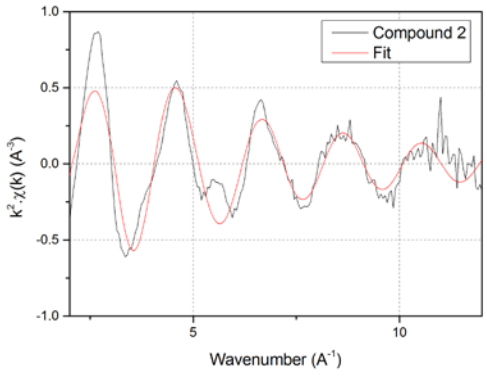

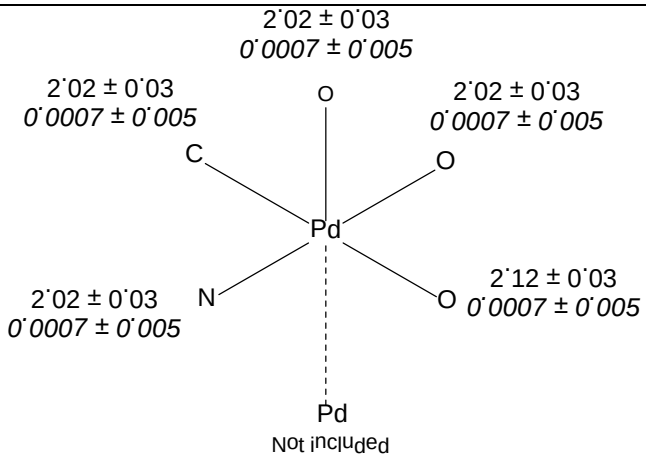

S02	= 0.77
CN	= 8.3
E0	= 6.53
R-factor	= 0.033

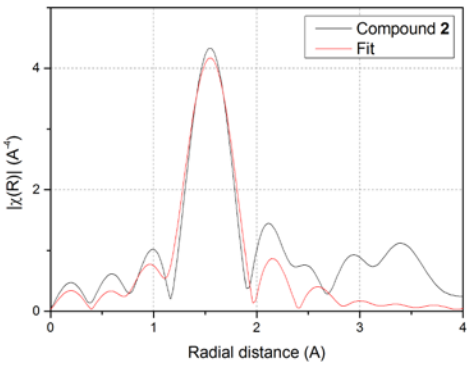

Figure S6. Fit of structure **2** (first shell of solution data), R-range 1-2, using Demeter. Bond distances are in Å in normal font, Debye-Waller factors are in italic font. The poor solution data quality prevents fitting with the longer Pd-Pd bond included.

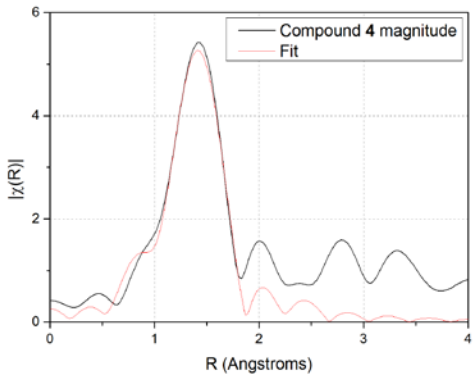

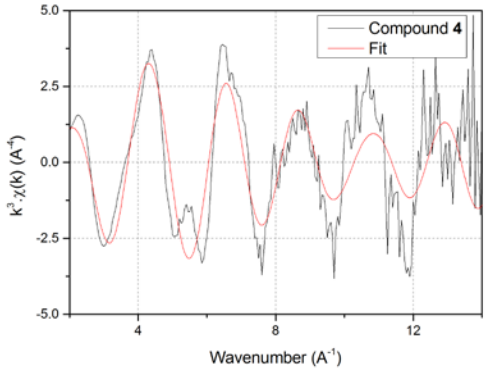

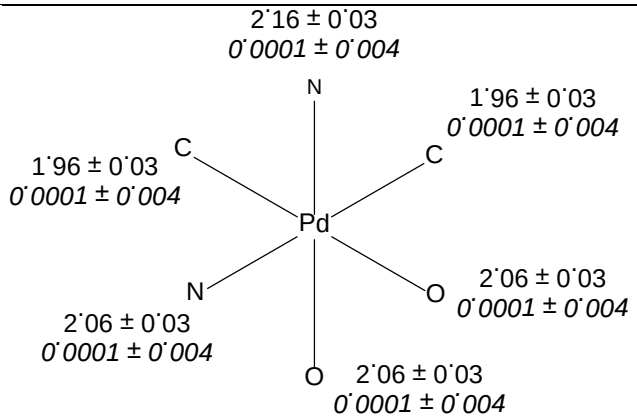

S02	= 0˙77
CN	= 6˙5
E0	= 7˙17 ± 2˙30
R factor	= 0˙007

Figure S7. Fit of structure **4** (first shell only), R-range 1-2, using Demeter. Bond distances are in Å in normal font, Debye-Waller factors are in italic font.

Electrochemical experiments.

All samples were degassed with Ar for at least 30 minutes prior to the experiments. Cyclic voltammograms were recorded in MeCN/0.1 M $^{n}Bu_4NPF_6$ on a CHI760C potentiostat (CH Instruments, Austin, Texas) with a glassy carbon (GC) disc as working electrode (diameter d = 2.5 mm; Windsor Scientific, Slough), and Pt-wire as reference and counter electrodes respectively. A solution of complex **1** was dissolved in acetonitrile to furnish a concentration of 1 mM. Potentials were calibrated to an internal $[Fc]^+/[Fc]$ reference (ferrocence concentration = 1 mM). Control experiments were performed with a boron-doped diamond electrode (d = 2.5 mm; Windsor Scientific, Slough) and single-crystal Au(111) electrodes (d = 3 mm). The latter were fabricated in-house using Clavillier's method.[12]

Raw data files for the electrochemical experiments are deposited on a digital depository, which is accessible via the following link: http://dx.doi.org/10.5281/zenodo.28488

CV of complex **1** measured with GC electrode in a low potential window is shown in article.

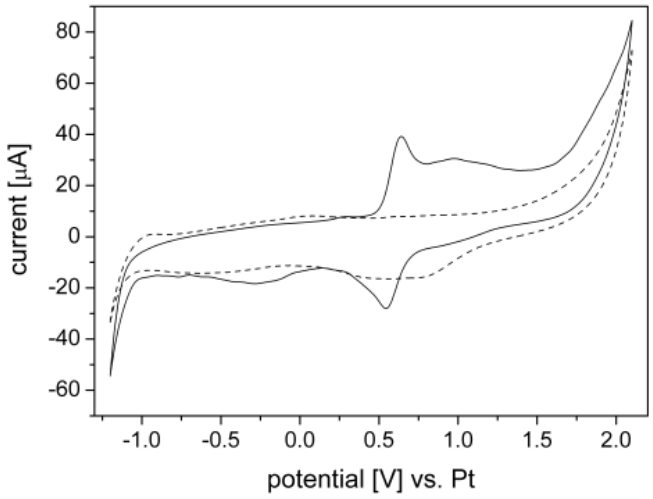

Figure S8. Solid line: CV of complex **1** measured with a Au(111) working electrode. Dotted line: background scan.

The CV features shown in Fig. S8 is representative of complex **1**. Under these conditions, CV response is stable between scans. However, the CV response of complex **1** is affected by the electrode material, suggesting that the redox species involved can react with the electrode surface (Figures S8 and S9).

However, the number of redox transitions seems to be the same, indicating that the overall redox chemistry remains the same.

Theoretical calculations. DFT and CM5 calculations were performed using Gaussian'09 program versions C.01 and D.01, respectively.[13] The energy of each compound was optimised using the WB97XD functional with the Def2TZVP basis set applied at Pd and 6-31G(d,p) for all other elements, and CPCM solvent correction for dichloroethane. HOMO and LUMO diagrams were generated using Gaussview 5.0 program.

Outputs for the calculations were deposited within a digital repository, and can be accessed *via* the following links:

Complex **1**: https://spectradspace.lib.imperial.ac.uk:8443/handle/10042/195427

Complex **2**: https://spectradspace.lib.imperial.ac.uk:8443/handle/10042/195428

Complex **3**: https://spectradspace.lib.imperial.ac.uk:8443/handle/10042/195429

Complex **4**: https://spectradspace.lib.imperial.ac.uk:8443/handle/10042/195430

References

1 I. Aiello, A. Crispini, M. Ghedini, M. La Deda and F. Barigelletti, *Inorg. Chim. Acta*, 2000, **308**, 121-128.

2 P. Jolliet, M. Gianini, A. von Zelewsky, G. Bernardinelli and H. Stoeckli-Evans, *Inorg. Chem.* 1996, **35**, 4883-4888.

3 J. M. Racowski, A. R. Dick and M. S. Sanford, *J. Am. Chem. Soc.* 2009, **131**, 10974-10983.

4 D. C. Powers and T. Ritter, *Nat. Chem.* 2009, **1**, 302-309.

5 G.M. Sheldrick, *Acta Cryst*.: *Sect. A*, 2008, **A64**, 112-122.

6 [INEVIG] A. Berger, J.-P. Djukic, M. Pfeffer, J. Lacour, L. Vial, A. de Cian and N. Kyritsakas-Gruber, *Organometallics* 2003, **22**, 5243–5260.

7 [MIXKUZ] A. Berger, A. de Cian, J.-P. Djukic, J. Fischer and M. Pfeffer, *Organometallics*, 2001, **20**, 3230–3240.

8 Though neither report makes any mention of how the nitrogen positions were located, the lack of any disorder, the "reasonable" nature of the thermal parameters, and (where applicable) the preference of $Cr(CO)_3$ units for π-bonding to phenyl rings rather than pyridyl rings suggest that the nitrogen positions are reliable.

9 X-ray crystallography identifies electron density, and in electron density terms there is not much of a difference between a carbon atom and a nitrogen atom. In order to identify a nitrogen centre purely on the basis of X-ray crystallography requires good quality data and careful analysis.

10 A. R. Dick, J. W. Kampf and M. S. Sanford, *J. Am. Chem. Soc.* 2005, **127**, 12790-12791.

11 B. Ravel and M. Newville, *J. Synchrotron Rad*. 2005, **12**, 537-541; M. Newville, *J. Synchrotron Rad*. 2001, **8**, 322-324.

12 J. Clavilier, R. Fauré, G. Guinet, and R. Durand, *J. Electroanal. Chem*. 1983, **107**, 181.

13 Frisch, M. J.; Trucks, G. W.; Schlegel, H. B.; Scuseria, G. E.; Robb, M. A.; Cheeseman, J. R.; Scalmani, G.; Barone, V.; Mennucci, B.; Petersson, G. A.; Nakatsuji, H.; Caricato, M.; Li, X.; Hratchian, H. P.; Izmaylov, A. F.; Bloino, J.; Zheng, G.; Sonnenberg, J. L.; Hada, M.; Ehara, M.; Toyota, K.; Fukuda, R.; Hasegawa, J.; Ishida, M.; Nakajima, T.; Honda, Y.; Kitao, O.; Nakai, H.; Vreven, T.; Montgomery, Jr., J. A.; Peralta, J. E.; Ogliaro, F.; Bearpark, M.; Heyd, J. J.; Brothers, E.; Kudin, K. N.; Staroverov, V. N.; Kobayashi, R.; Normand, J.; Raghavachari, K.; Rendell, A.; Burant, J. C.; Iyengar, S. S.; Tomasi, J.; Cossi, M.; Rega, N.; Millam, J. M.; Klene, M.; Knox, J. E.; Cross, J. B.; Bakken, V.; Adamo, C.; Jaramillo, J.; Gomperts, R.; Stratmann, R. E.; Yazyev, O.; Austin, A. J.; Cammi, R.; Pomelli, C.; Ochterski, J. W.; Martin, R. L.; Morokuma, K.; Zakrzewski, V. G.; Voth, G. A.; Salvador, P.; Dannenberg, J. J.; Dapprich, S.; Daniels, A. D.; Farkas, Ö.; Foresman, J. B.; Ortiz, J. V.; Cioslowski, J.; Fox, D. J. Gaussian, Inc., Wallingford CT, 2009.